

DUAL LINEAR POLARIZATION RECONFIGURABLE PATCH ANTENNAS FOR LOWER 5G FREQUENCY BAND

ABDELLAH ATTALHAOUI, ABDELHAK BENDALI, ABID-REDA EI WARDI, MOHAMED HABIBI

Laboratory of Electronic System, Information Processing, Mechanics and Energetic, Ibn Tofail University
Kenitra, Morocco

E-mail: abdellah.attalhaoui@gmail.com

ABSTRACT

Linear polarization reconfigurable patch antennas for 5G application are presented in this paper. The first type is U-shaped antenna which has been proposed and analyzed and can switch among two symmetric polarizations. The second type is Y-shaped antenna which has been analyzed and can switch among two orthogonal polarizations. The two types of antennas can generate the polarization diversity without affecting the other performances such as the radiation pattern and the frequency. These types of antennas are required for wireless communication systems because they can avoid the fading loss and increase the channel capacity. To achieve the linear polarization reconfigurability, two diodes are integrated into microstrip feed. For both states of operation of antennas, the resonant frequency was determined to be between (3.4–3.6) GHz. The simulated results of reflection coefficient and gain are carried out using HFSS (high frequency structural simulator) and CST (computer simulation technology) software. The operation frequency, the simple structure, and good gain make these antennas good candidates for 5G communication.

Keywords: *Polarization Reconfigurable Patch Antenna, U-Shaped Antenna, Y-Shaped Antenna, HFSS, CST*

1. INTRODUCTION

As a result of the development of technology and increases number of users in wireless communication system, there is necessity to use reconfigurable patch antennas. They can alleviate multipath fading loss, enhance channel capacity by frequency reuse and increase the quality of the signal [1]. The reconfigurability functions of the antenna are radiation pattern [2, 3], frequency band [4, 5] and polarization [6, 7]. Frequency reconfigurable antennas allow to move dynamically or continuously from one frequency band to another or in a range of frequencies, respectively. On the other hand, the pattern reconfigurable antennas provide beam steering in a desired direction. While the polarization reconfigurable antennas capable to modify the polarization characteristics in real time. In order to ensure reconfigurability, various techniques include optical [8-10], physical [11-13], material [14-16], and electrical [17-21] have been suggested. The electrical technique is most widely used, which uses switching devices like, varactors diodes [17], RF micro electro mechanical systems (MEMS) [18], and PIN diodes [19-21]. Because of

their low price and their acceptable performance, the PIN diodes are suitable for reconfigurable antennas. Several antennas have been developed to achieve the polarization reconfigurability. These antennas have the advantage of activating two or more polarizations by employing one resonator and this leads to minimizing a large amount of space. They have ability to change the sense of polarization between Left-hand circular polarization (LHCP) and Right-hand circular polarization (RHCP) or between linear polarizations (LPs). To control the polarization states, many antennas are created by inserting PIN diodes. In [22] the antenna mainly consists of a slot antenna and a polarizer, both LHCP and RHCP are obtained by adjusting the states of two PIN diodes. Furthermore, a square patch with a semicircular slot is realized [23], by utilizing two PIN diodes, the antenna can switch its polarizations between LHCP and RHCP. On other hand, the number of papers that have worked on multi-linear polarization is insufficient. In [24], a square patch antenna with Y-shaped feed structure is proposed, the orthogonal and horizontal polarizations controlled by the states of two diodes. A circular patch antenna with four shorting posts

and four PIN diodes was proposed in [25]. Depending on the states of four diodes, four linear polarizations rotated 45° are achieved. While in [26], a square-ring antenna with two shorting stubs and two PIN diodes is proposed. The state of two diodes can altered between two linear orthogonal polarizations. In this paper, two microstrip patch antennas with linear polarization diversity are suggested. These antennas consist of a square patch antenna with U-shaped feed, and Y-shaped feed. Two PIN diodes are inserted into feed line of both antennas to provide reconfiguration between two linear polarizations. By tuning two diodes on and off, the U-shaped antenna and Y-shaped antenna can generate two linear polarizations symmetric to each other and two linear polarizations orthogonal to each other, respectively, without influencing the radiation pattern and the resonance frequency. The frequency band (3.4–3.6) GHz, the simple structure, and gain of 3.08 to 3.88 dB make these antennas appropriate for 5G communication.

2. EQUIVALENT CIRCUIT MODEL OF PIN DIODE

In order to achieve the polarization reconfigurability, the (BAP65-02, 115) diodes are used for switching. For ON state, the PIN diode can modeled as a series combination of resistor $R_s = 1\Omega$, and inductor $L_s = 0.6nH$. For OFF state, it can modeled as a parallel combination of capacitor $C_p = 0.5pF$ and resistor $R_p = 20k\Omega$ in series connection with inductor $L_s = 0.6nH$. The equivalent circuit of the PIN diode at each state is illustrated in Fig. 1.

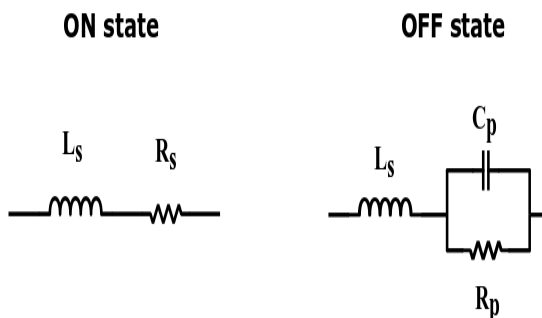


Figure 1: PIN DIODE model in OFF state and ON state

3. PATCH ANTENNA WITH U-SHAPED FEED

The geometry of the reconfigurable patch antenna is illustrated in Fig. 2. It consists of a square radiating patch, U-shaped feed, and two PIN diodes. The

antenna structure is designed on a FR4 substrate with dielectric constant $\epsilon_r = 4.4$, loss tangent of 0.02, and thickness $h=1.6mm$. The radiating patch has dimensions of $19.5mm \times 19.5mm$ and can be calculated using the following equations:

$$W = \frac{c}{2f_r} \sqrt{\frac{2}{\epsilon_r + 1}} \tag{1}$$

$$L = \frac{c}{2f_r \sqrt{\epsilon_{reff}}} - 2\Delta L \tag{2}$$

$$\epsilon_{reff} = \frac{\epsilon_r + 1}{2} + \frac{\epsilon_r - 1}{2} \sqrt{1 + \frac{12h}{W}} \tag{3}$$

$$\Delta L = 0.412h \frac{(\epsilon_{reff} + 0.3)(W/h + 0.264)}{(\epsilon_{reff} - 0.258)(W/h + 0.8)} \tag{4}$$

Where W and L are the width and the length of the patch, respectively, ϵ_r is the relative permittivity, f_r is the resonant frequency, ϵ_{reff} is the effective dielectric constant and c is the velocity of light.

The size of feed line is selected to present a characteristic impedance of 50Ω . A distance g was kept between U-shaped feed and square radiating patch. Two PIN diodes are integrated into U-shaped feed. Both the left and right branchlines of U-shaped feed have the width of d and contain a length of H .

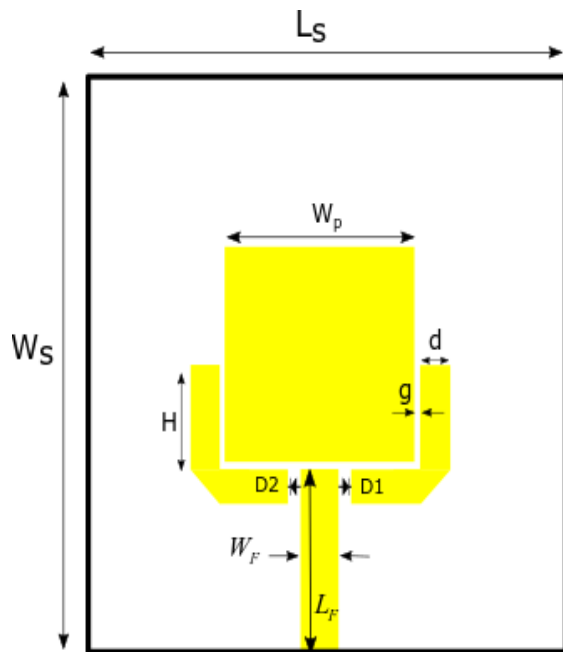


Figure 2: Geometry of U-shaped antenna

The U-shaped proposed antenna was simulated using High Frequency Structure Simulator (HFSS). To understand the influence of antenna parameters on the reflection coefficient, a parametric study is carried on the gap g , the length H , and width d of the branchline of the U-shaped feed when PIN diode 1 tuned ON and PIN diode 2 tuned OFF (state 1).

The sensitivity of the reflection coefficient to variation in the gap g is simulated in Fig. 3.

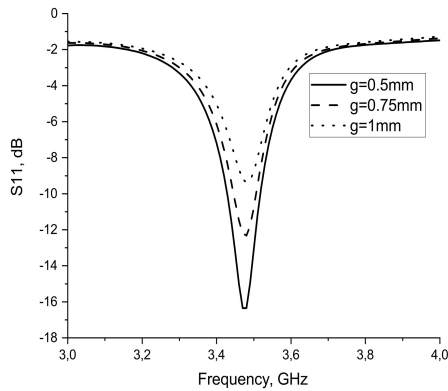


Figure 3: Simulated reflection coefficient at $d=2$ mm, $H=9.5$ mm, and different values of g

It is clear from the simulation that the reflection coefficient decreases when g is increased.

Fig. 4 shows the length H effect in terms of reflection coefficient. It can be seen from the simulation that the center of the operation frequency increases when H is increased.

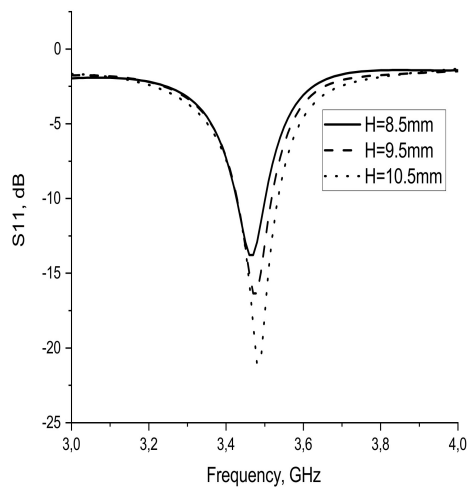


Figure 4: Simulated reflection coefficient at $g=0.5$ mm, $d=2$ mm, and different values of H

The reflection coefficient with different values of the width d is illustrated in Fig. 5. As can be seen, when d increases, the center of the operation frequency moves towards to the lower frequency.

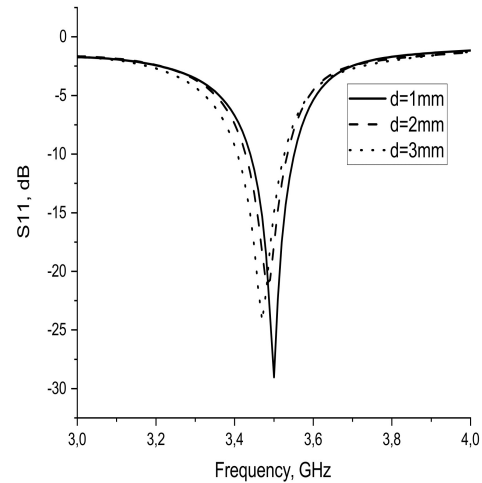


Figure 5: Simulated reflection coefficient at $g=0.5$ mm, $H=10.5$ mm, and different values of d

The optimized parameters of U-shaped antenna are listed in Table 1

Table 1: Parameters of U- shaped antenna.

Parameters	Value (mm)
$L_s=W_s$	47
W_p	19.5
d	1
H	10.5
g	0.5
W_f	3.0589
L_f	11.7424

Fig. 6(a) and (b) describes the surface current distributions of the proposed antenna at 3.5 GHz when it is worked in state 1 (diode 1 is on, and diode 2 is off) and in state 2 (diode 1 is off, and diode 2 is on), respectively. It is clear from this simulation that for two states of operation, the current distributions symmetric to each other. For this reason, the U-shaped proposed antenna has the ability to carry out the polarization diversity.

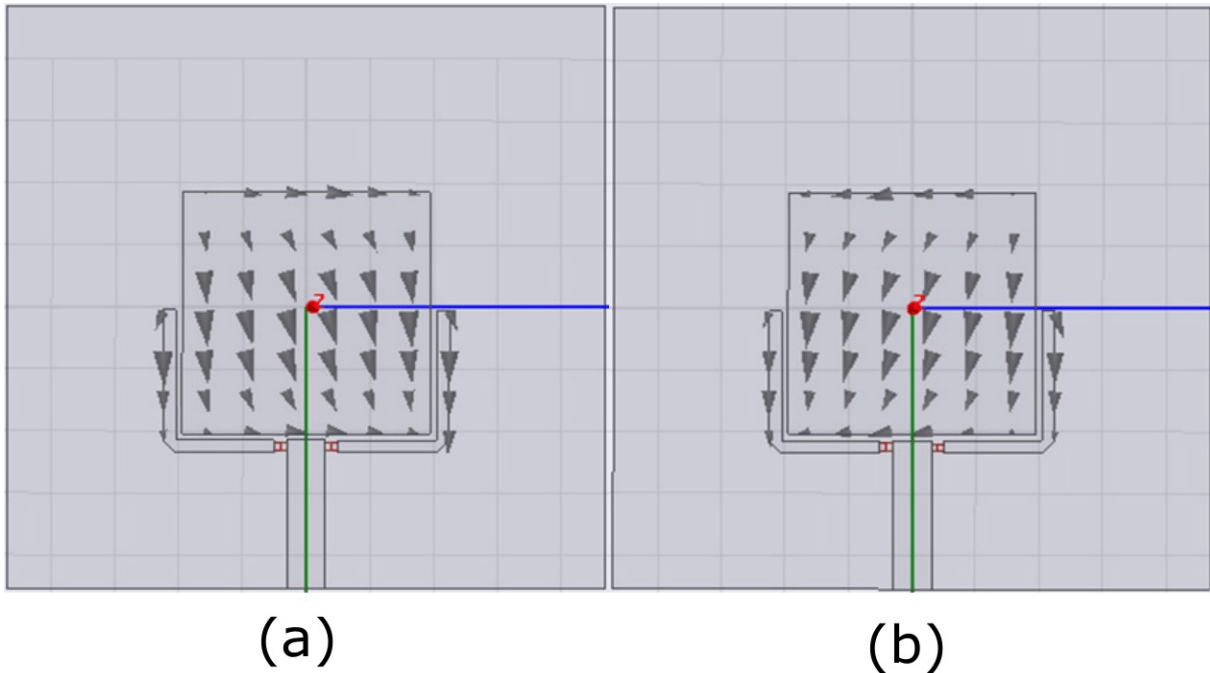


Figure 6: Simulated current distributions of U-shaped antenna: (a) state 1 and (b) state 2

The optimized values of the proposed antenna obtained from HFSS software have been employed to be used in CST Microwave Studio simulation software.

The simulated reflection coefficient versus frequency results using both HFSS and CST software are presented in Fig. 7. From the figure, it can be observed that, for two different states that have been carried out using the same software (HFSS or CST), S11 picks at the same resonance frequency.

The reflection coefficient of -29 dB, and -29.3 dB for state 1 and state 2, respectively are obtained from HFSS at the frequency 3.5 GHz, while the reflection coefficient of -12.2 dB for two states is obtained from CST at the frequency 3.45 GHz. By modifying the state of two diodes, the resonance frequency was maintained using the same software, which is an added value of this antenna. The discrepancies in reflection coefficient obtained with HFSS and CST due to difference between their theoretical models, specifically HFSS is based on finite element method (FEM), while CST is based on finite integration techniques (FIT).

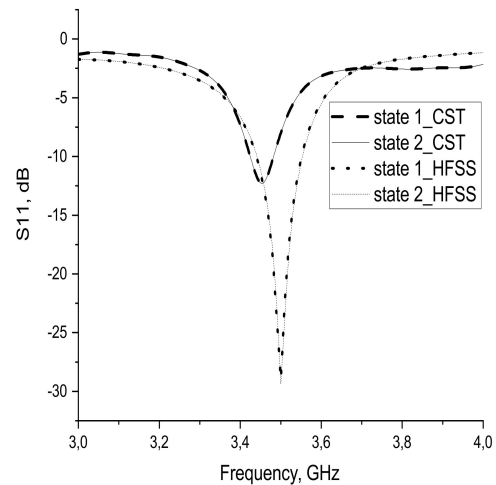


Figure 7: Comparison of S11 from HFSS and CST in state 1 and state 2 at $d=1$ mm, $H=10.5$ mm, and $g=0.5$ mm

Fig. 8(a) and (b) shows the simulated gain in $\phi = 0^\circ$ plane and $\phi = 90^\circ$ plane at 3.5 GHz when U-shaped antenna operates in state 1 and state 2, respectively. The maximum gain, using HFSS software, was 3.77 dB for state 1, while it was 3.88 dB for state 2. On other hand, the maximum gain, using CST software, was 3.46 dB for both states. As can be seen, the proposed antenna has a unidirectional pattern and by changing the states of two diodes, the direction of radiation pattern in

each plane was almost conserved by using the same antenna. software, which is another advantage of this

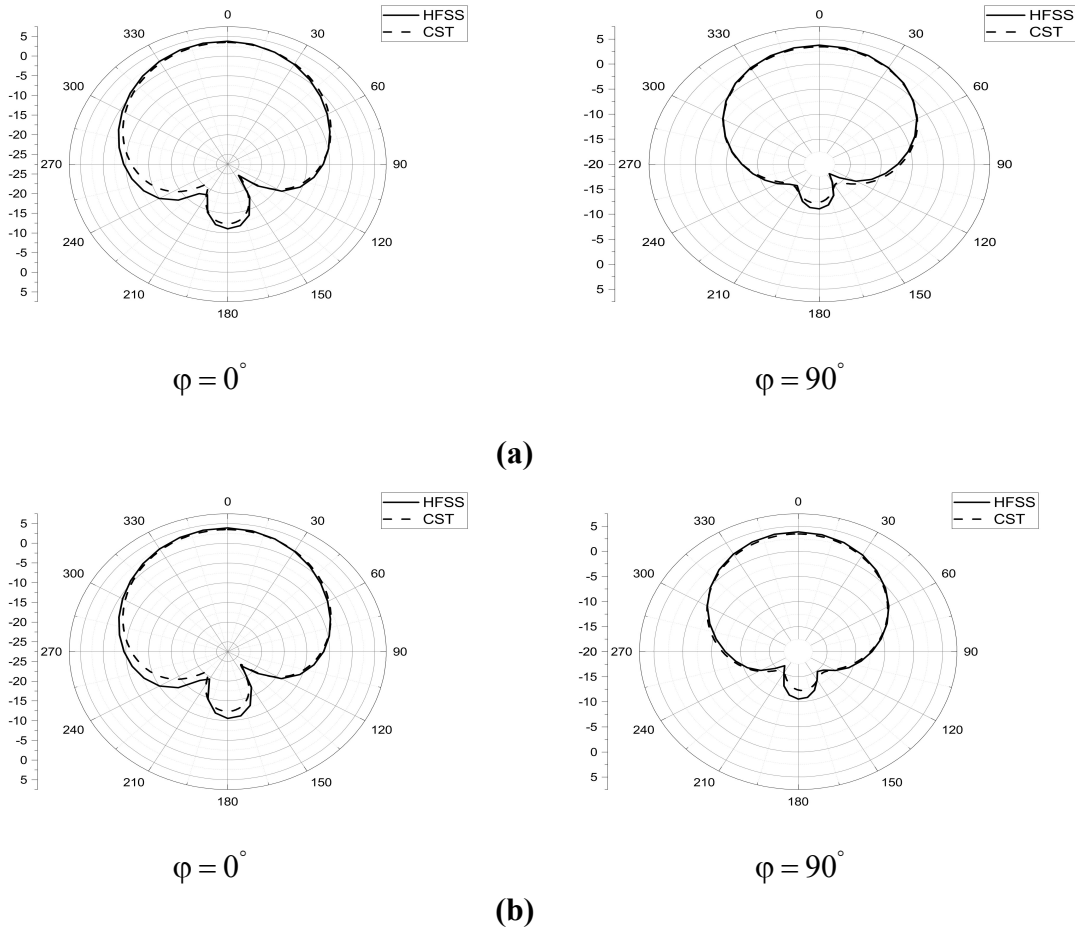


Figure 8: Simulated radiation patterns of U-shaped antenna (a) state1 (b) state 2

4. PATCH ANTENNA WITH Y-SHAPED FEED

The Y-shaped antenna has been proposed in [24] to operate at 2.51 GHz. The geometry of this antenna is illustrated in Fig. 9. We keep the same characteristics of substrate, the feed of 50Ω , and the dimensions of radiating patch that have been used in U-shaped antenna. Also the same types of two PIN diodes (BAP65-02, 115) are integrated into Y-shaped feed. The two orthogonal branchlines of Y-shaped feed have the width of d and length of H . The proposed antenna has been analyzed using HFSS software when PIN diode 1 tuned ON and PIN diode 2 tuned OFF. There are various parameters of the Y-shaped antenna which have significant effect on the reflection coefficient including the gap g , the width d , and the length H of the branchline of the Y-shaped feed.

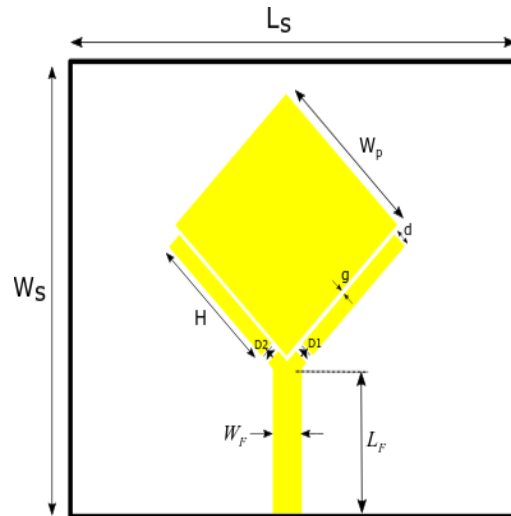


Figure 9: Geometry of U-shaped antenna

The reflection coefficient with different values of the width d is illustrated in Fig. 10. As can be seen, the reflection coefficient increases when d is increased

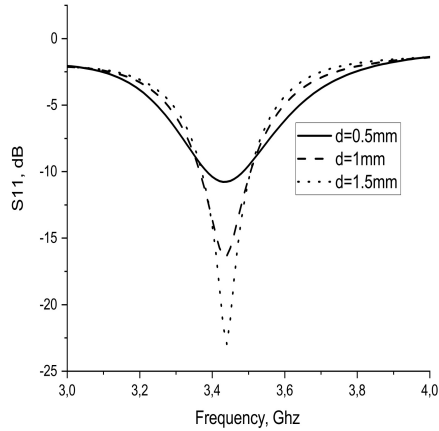


Figure 10: Simulated reflection coefficient at $g=0.5$ mm, $H=16.2$ mm and different values of d

Fig. 11 shows the impact of H on the reflection coefficient. It can be observed from this figure that when H increases, the operating frequency shifts to the higher frequency and $H=18.2$ mm offers the desired frequency of 3.5 GHz.

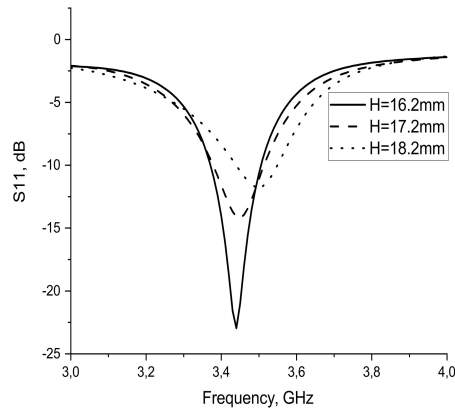


Figure 11: Simulated reflection coefficient at $g=0.5$ mm, $d=1.5$ mm and different values of H

The reflection coefficient with different values of the gap g is illustrated in Fig. 12.

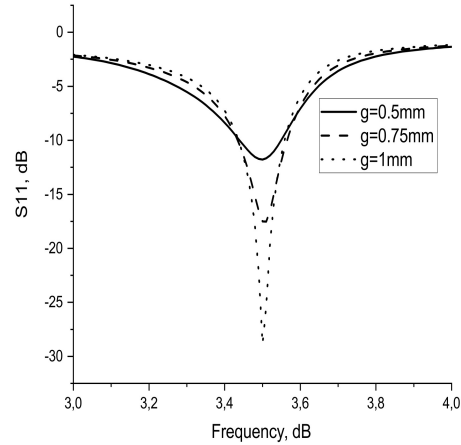


Figure 12: Simulated reflection coefficient at $H=18.2$ mm, $d=1.5$ mm and different values of g

It is clear from the simulation that the reflection coefficient increases when g is increased and it is found that $g=1$ mm gives best results in terms of reflection coefficient.

The optimized parameters of Y-shaped antenna are listed in Table 2.

Table 2: Parameters of Y- shaped antenna.

Parameters	Value (mm)
$L_s=W_s$	47
W_p	19.5
d	1.5
H	18.2
g	1
W_f	3.0589
L_f	11.7424

Fig. 13(a) and (b) describes the surface current distributions of the proposed antenna at 3.5 GHz when it is worked in state 1 and in state 2, respectively. It is clear from this simulation that for two states of operation, the current distributions orthogonal to each other and that makes it able to carry out the polarization diversity.

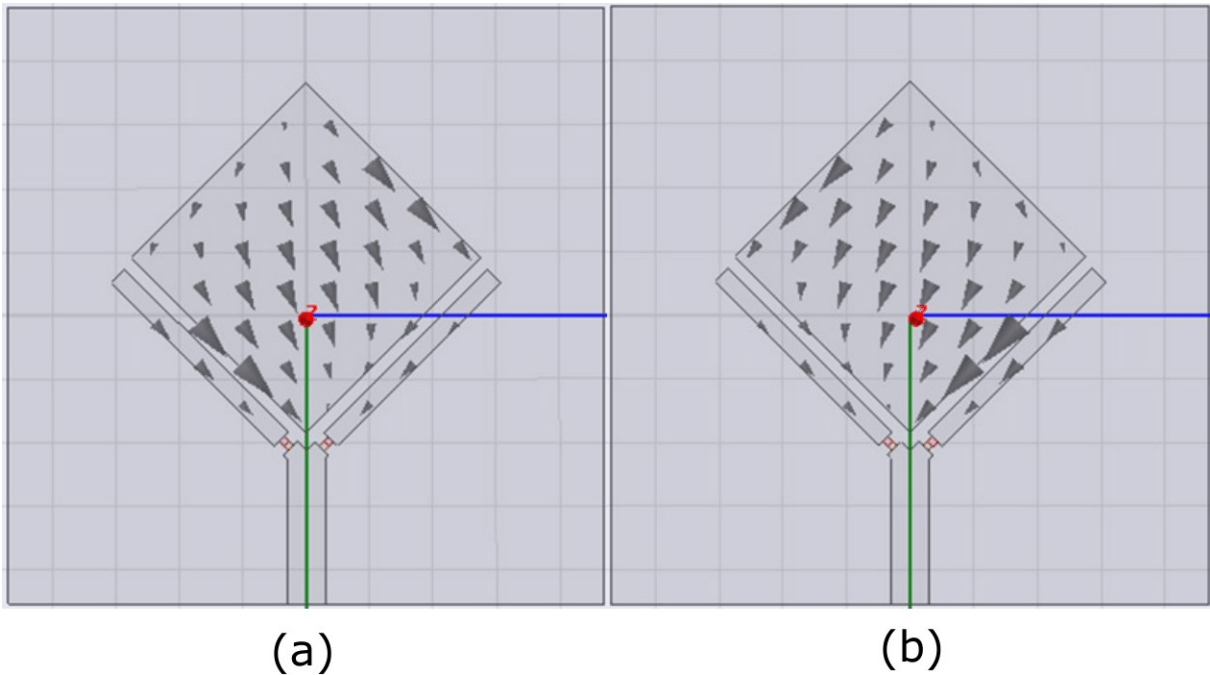


Figure 13: Simulated current distributions of Y-shaped antenna: (a) state 1 and (b) state 2

Fig.14 shows the simulated reflection coefficient versus frequency results for state 1 (diode 1 is on, and diode 2 is off) and state 2 (diode 1 is off, and diode 2 is on) using HFSS and CST software. The simulated results show that the resonance frequency for both states using HFSS software are 3.5 GHz with $S_{11} = -28.8$ dB, and $S_{11} = -27.4$ dB for state 1 and state 2, respectively, while in the case of CST software, the resonance frequency for both states are 3.42 GHz with $S_{11} = -17.2$ dB. As can be seen, by controlling the states of two diodes, the resonance frequency was conserved by using the same software, which is an added value of this antenna. The slight differences in reflection coefficient obtained with HFSS and CST due to difference between their computations models.

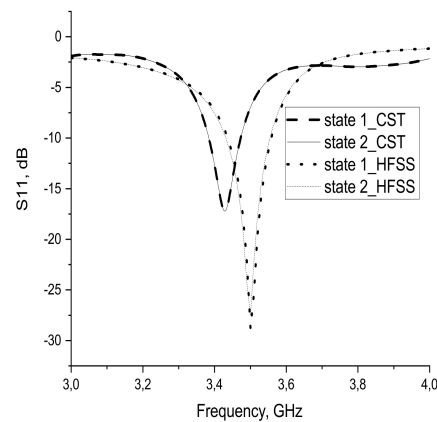


Figure 14: Comparison of S_{11} from HFSS and CST in state 1 and state 2 at $d=1.5$ mm, $H=18.2$ mm, and $g=1$ mm

Fig. 15(a) and (b) shows the simulated gain in $\phi=0^\circ$ and $\phi=90^\circ$ planes at 3.5 GHz when antenna operates in state 1 and state 2, respectively. The maximum gain, using HFSS software, was 3.6 dB for state 1, while it was 3.67 dB for state 2. On other hand, the maximum gain, using CST software, was 3.08 dB for both states. As can be seen, the proposed antenna has a unidirectional radiation pattern and the radiation pattern direction for the two states of operation of antenna in each plane was maintained using the same software,

which means that the antenna is not affected by changing the states of two PIN diodes.

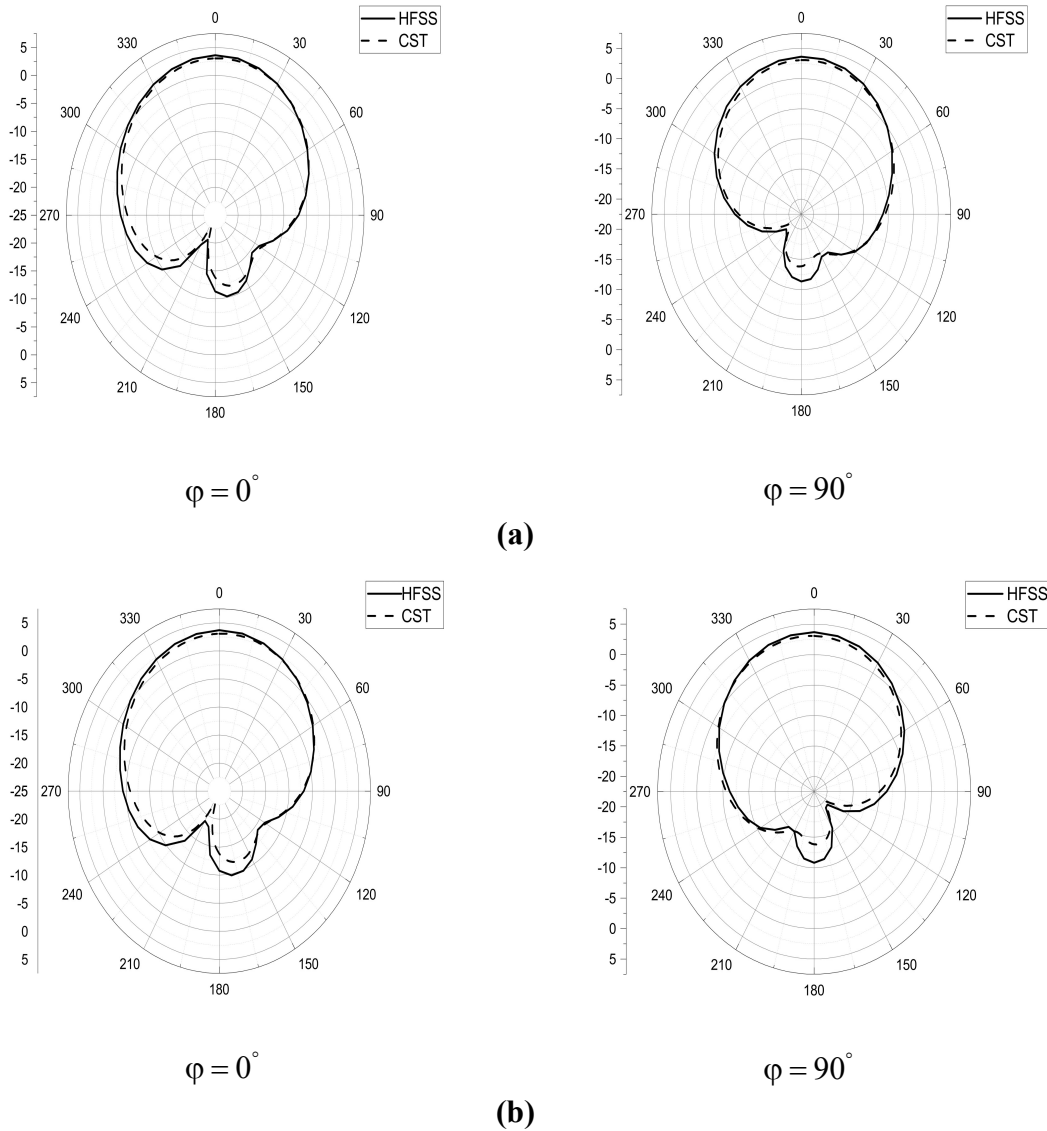


Figure 15: Simulated radiation patterns of Y-shaped antenna (a) state1 (b) state 2

Finally, some comparisons between the proposed polarization reconfigurable antennas and other antennas reported in the literature are given in Table 3. It is clear that the two proposed antenna

have smaller sizes, simple structures and fewer switches.

Table 3: Comparison between the proposed antennas and reported polarization reconfigurable antennas.

Ref.	Size (mm ²)	Switching Element	Design Complexity	Frequency (GHz)	Polarization States
[20]	70 × 70 × 1.6	2 PIN diodes	Square patch with Y-shaped feed	2.5	LHCP- RHCP
[21]	50 × 50 × 1.6	4 PIN diodes	Square patch with a diagonal-shaped slot	2.35	LP- LHCP- RHCP
[23]	34 × 34 × 3.2	2 PIN diodes	Square patch with a semicircular slot	3.4	LHCP- RHCP
[24]	70 × 70 × 1.6	2 PIN diodes	Square patch with Y-shaped feed	2.51	Two orthogonal LPs
This work	47 × 47 × 1.6	2 PIN diodes	<ul style="list-style-type: none"> • Square patch with Y-shaped feed • Square patch with U-shaped feed 	3.5	Two orthogonal LPs Two symmetric LPs

5. CONCLUSION

Linear polarization reconfigurable antennas for 5G application have been presented. The first one consists of a square radiating patch and U-shaped feed, while the last one consists of a square radiating patch and Y-shaped feed. By controlling the state of two diodes, the U-shaped antenna and Y-shaped antenna can switch among two symmetric polarizations, and two orthogonal polarizations, respectively, without affecting the other performances such as the radiation pattern and the resonance frequency. Because of their ability to enhance channel capacity by frequency reuse and to avoid the fading loss caused by multipath effects, the proposed antennas are suitable for wireless communication systems.

REFERENCES:

- [1] N. Ojaroudi Parchin, H. Jahanbakhsh Basherlou, Y. I. A. Al-Yasir, R. A. Abd-Alhameed, A. M. Abdulkhaleq, and J. M. Noras, "Recent developments of reconfigurable antennas for current and future wireless communication systems," *Electronics*, vol. 8, no. 2, pp. 1-17, 2019.
- [2] Z. Xu and C. Deng, "High-isolated MIMO antenna design based on pattern diversity for 5G mobile terminals," *IEEE Antennas and Wireless Propagation Letters*, vol. 19, no. 3, pp. 467-471, March 2020.
- [3] S. Singhal, "A symmetrically fed trapezoidal superwideband pattern diversity antenna," *Optik*, vol. 231, pp. 166358, 2021.
- [4] I. A. Shah, S. Hayat, A. Basir, M. Zada, S. A. A. Shah, and S. Ullah, "Design and analysis of a hexa-band frequency reconfigurable antenna for wireless communication," *AEU-International Journal of Electronics and Communications*, vol. 98, pp. 80-88, January 2019.
- [5] K. Moradi, A. Pourziad, and S. Nikmehr, "A frequency reconfigurable microstrip antenna based on graphene in Terahertz Regime," *optik*, vol. 231, pp. 166201, 2021.
- [6] M. Saravanan and M. J. S. Rangachar, "Polarization Reconfigurable Square Patch Antenna for Wireless Communications," *Advanced Electromagnetics*, vol. 7, no. 4, pp. 103-108, Sep. 2018.
- [7] Z. C. Hao, K. K. Fan, and H. Wang "A planar polarization reconfigurable antenna," *IEEE Trans. Antennas Propag.*, vol. 65, no. 4, pp. 1624-1632, April 2017.
- [8] S.-H. Zheng, X.-Y. Liu, M.M. Tentzeris, "A novel optically controlled reconfigurable antenna for cognitive radio systems," In *Proceedings of the IEEE Antennas and Propagation Society International Symposium (APSURSI)*, Memphis, TN, USA, 6-11 July 2014; pp. 1246-1247
- [9] V. A. Manasson, L.S. Sadovnik, V. A. Yepishin, D. Marker, "An optically controlled millimeter wave beam-steering antenna based on a novel architecture," *IEEE Trans. Microw. Theory Tech.* 1997, 45, 1497-1500.
- [10] I. F. Da Costa, A. Cerqueira, D. H. Spadoti, L. G. da Silva, J. A. J. Ribeiro, S. E. Barbin, "Optically controlled reconfigurable antenna array for mm-wave applications," *IEEE Antennas Wirel. Propag. Lett.* 2017, 16, 2142-2145.
- [11] Y. TAWK, J. COSTANTINE, C. G. CHRISTODOULOU, "A frequency reconfigurable rotatable microstrip antenna design," In : 2010 IEEE Antennas and

- Propagation Society International Symposium. IEEE, 2010. p. 1-4.
- [12] P. Mathur, G. Madanan, and S. Raman, "Mechanically frequency reconfigurable antenna for WSN, WLAN, and LTE 2500 based Internet of Things applications," *Int. J. RF Microw. Comput.-Aided Eng.*, vol. 31, no. 2, Feb. 2021, p. e22318.
- [13] I. T. Nassar, H. Tsang, D. Bardroff, C. P. Lusk, and T. M. Weller, "Mechanically reconfigurable, dual-band slot dipole antennas," *IEEE Transactions on Antennas and Propagation*, vol. 63, no. 7, pp. 3267–3271, 2015.
- [14] S. Wang, L. Zhu, and W. Wu, "A novel frequency-reconfigurable patch antenna using low-loss transformer oil," *IEEE Trans. Antennas Propag.*, vol. 65, no. 12, pp. 7316–7321, Dec. 2017
- [15] J. L. Salazar-Cerreno, Z. Qamar, S. Saeedi, B. Weng, and H. S. Sigmarsson, "Frequency agile microstrip patch antenna using an anisotropic artificial dielectric layer (AADL): Modeling and design," *IEEE Access*, vol. 8, pp. 6398–6406, 2020.
- [16] L.-R. Tan, R.-X. Wu, C.-Y. Wang, and Y. Poo, "Magnetically Tunable Ferrite Loaded SIW Antenna," *IEEE Antennas Wireless Propag. Lett.*, vol. 12, pp. 273–275, 2013
- [17] R. Jeanty and S.-Y. Chen, "A low-profile polarization-reconfigurable cavity antenna based on partially reflective surface," in *Radio-Frequency Integration Technology (RFIT), 2017 IEEE International Symposium*, pp. 226–228, 2017.
- [18] M. Wright, M. Ali, W. Baron, J. Miller, J. Tuss, and D. Zeppetella, "Effect of bias traces and wires on a MEMS reconfigurable pixelated patch antenna," in *Antennas and Propagation (APSURSI), 2016 IEEE International Symposium*, pp. 1429–1430, 2016.
- [19] B. Liu, J. Qiu, C. Wang, and G. Li, "Pattern-Reconfigurable Cylindrical Dielectric Resonator Antenna Based on Parasitic Elements," *IEEE Access*, Vol. 5, pp. 25584–25590, November 2017.
- [20] S. W. Lee and Y. J. Sung, "Reconfigurable rhombus-shaped patch antenna with Y-shaped feed for polarization diversity," *IEEE Antennas Wireless Propag. Lett.*, vol. 14, pp. 163–166, 2015
- [21] M. Saravanan, M. J. S. Rangachar, "Polarization Reconfigurable Square Patch Antenna for Wireless Communications," *Advanced Electromagnetics*, vol. 7, no. 4, pp. 103–108, 2018.
- [22] W. Li, S. Gao, Y. Cai, Q. Luo, M. Sobhy, G. Wei, J. Xu, J. Li, C. Wu, and Z. Cheng, "Polarization reconfigurable circularly polarized planar antenna using switchable polarizer," *IEEE Trans. Antennas Propag.*, vol. 65, no. 9, pp. 4470–4477, Sep. 2017.
- [23] Y. I. A. Al-Yasir, A. S. Abdullah, N. Ojaroudi Parchin, R.A. Abd-Alhameed, and J.M. Noras, "A new polarization-reconfigurable antenna for 5G applications," *Electronics*, vol. 7, no. 11, pp. 1–9, 2018.
- [24] S. W. Lee and Y. Sung, "A polarization diversity patch antenna with a reconfigurable feeding network," *Journal of electromagnetic engineering and science*, vol. 15, pp. 115–119, April 2015.
- [25] S. L. Chen, F. Wei, P. Y. Qin, Y. J. Guo, and X. Chen, "A multi-linear polarization reconfigurable unidirectional patch antenna," *IEEE Trans. Antennas Propag.*, vol. 65, no. 8, pp. 4299–4304, Aug. 2017.
- [26] Y. Sung, "Dual-band reconfigurable antenna for polarization diversity," *Int. J. Antennas Propag.*, pp. 1–7, 2018